REPORT SD-TR-85-78

Diffraction and the Radiometric Levitation of Carbon Aerosol Using a Nd:YAG Laser

Prepared by

A. B. PLUCHINO
Chemistry and Physics Laboratory
Laboratory Operations
The Aerospace Corporation
El Segundo, Calif. 90245

2 December 1985

Prepared for

SPACE DIVISION
AIR FORCE SYSTEMS COMMAND
Los Angeles Air Force Station
P.O. Box 92960, Worldway Postal Center
Los Angeles, Calif. 90009

This report was submitted by The Aerospace Corporation, El Segundo, CA 90245, under Contract No. F04701-85-C-0086 with the Space Division, P.O. Box 92960, Worldway Postal Center, Los Angeles, CA 90009-2960. It was reviewed and approved for The Aerospace Corporation by S. Feuerstein, Director, Chemistry and Physics Laboratory.

Lt Charles C. Neidhart was the project officer for the Mission-Oriented Investigation and Experimentation (MOIE) Program.

This report has been reviewed by the Public Affairs Office (PAS) and is releasable to the National Technical Information Service (NTIS). At NTIS, it will be available to the general public, including foreign nationals.

This technical report has been reviewed and is approved for publication. Publication of this report does not constitute Air Force approval of the report's findings or conclusions. It is published only for the exchange and stimulation of ideas.

Charles C Neidhart

CHARLES C. NEIDHART, Lt, USAF
MOIE Project Officer
SD/CGX

Joseph Hess

JOSEPH HESS, GM-15
Director, AFSTC West Coast Office
AFSTC/WCO OL-AB

UNCLASSIFIED

SECURITY CLASSIFICATION OF THIS PAGE (When Data Entered)

REPORT DOCUMENTATION PAGE	READ INSTRUCTIONS BEFORE COMPLETING FORM
1. REPORT NUMBER: SD-TR-85-78	2. GOVT ACCESSION NO.: AD-A167691
	3. RECIPIENT'S CATALOG NUMBER:
4. TITLE (and Subtitle): DIFFRACTION AND THE RADIOMETRIC LEVITATION OF CARBON AEROSOL USING A Nd:YAG LASER	5. TYPE OF REPORT & PERIOD COVERED:
	6. PERFORMING ORG. REPORT NUMBER: TR-0086(6945-08)-1
7. AUTHOR(s): A. B. Pluchino	8. CONTRACT OR GRANT NUMBER(s): F04701-85-C-0086
9. PERFORMING ORGANIZATION NAME AND ADDRESS: The Aerospace Corporation, El Segundo, Calif. 90245	10. PROGRAM ELEMENT, PROJECT, TASK AREA & WORK UNIT NUMBERS:
11. CONTROLLING OFFICE NAME AND ADDRESS: Space Division, Air Force Systems Command, Los Angeles, Calif. 90009	12. REPORT DATE: 2 December 1985
	13. NUMBER OF PAGES: 21
14. MONITORING AGENCY NAME & ADDRESS(if different from Controlling Office):	15. SECURITY CLASS. (of this report): Unclassified
	15a. DECLASSIFICATION/DOWNGRADING SCHEDULE:

16. DISTRIBUTION STATEMENT (of this Report)

Approved for public release; distribution unlimited.

17. DISTRIBUTION STATEMENT (of the abstract entered in Block 20, if different from Report)

18. SUPPLEMENTARY NOTES

19. KEY WORDS (Continue on reverse side if necessary and identify by block number)

Aerosol	Photophoresis
Diffraction	Radiometric Force
Levitation	Scattering

20. ABSTRACT (Continue on reverse side if necessary and identify by block number)

Experimental observations of highly absorbing carbon particles trapped in the beam of a Nd:YAG laser are presented. The physical mechanism responsible is discussed along with possible application and implications of this phenomenon.

DD FORM 1473 (FACSIMILE)

UNCLASSIFIED

SECURITY CLASSIFICATION OF THIS PAGE (When Data Entered)

CONTENTS

FIGURES

I. INTRODUCTION

Contd

In this work we report the levitation of highly absorbing particles with an infrared (IR) laser beam. This optical levitation is different from the radiation pressure phenomenon reported by Ashkin,[1,2] which applies to very weakly absorbing particulates. Suspension by radiation pressure requires weak absorbers since the photophoretic force[3,4] on a particle can be orders of magnitude higher than that due to photon momentum; therefore, it becomes impossible to stably trap an absorbing particle by the momentum of light alone except, possibly, in a vacuum. Photophoresis is the force on a particle due to the rebounding of ambient gas molecules with greater velocities from parts of the surface that are at a higher temperature. Absorbing nonspherical particles driven by such a force are known to migrate along complex paths. The motion can be along helical paths, complex orbits, or just irregular, random movement. For all of these paths, with the exception of the random motion, there is always a preferred direction, e.g., the axis of the orbit, due to some external factor such as the direction of the light, gravity, and applied electric and magnetic fields.

Spherical absorbing particles irradiated with a plane wave move in a straight line along the optical axis. Experimental evidence shows that the photophoretic force on a good absorber is normal to the surface irradiated and directed toward the center of the spherical particle. Using an Ar^+ laser with an intensity profile having a minimum at the center, i.e., the doughnut mode, Lewittes et al.[5] have stably levitated a single spherical drop of absorbing dye-impregnated glycerol. In other words, they have suspended a particle by letting it fall to the bottom of a light intensity well where the particle is nonuniformly heated so that the rebounding gas molecules produce an integrated force that keeps it centered and overcomes the gravitational influence.

Using a linearly polarized IR laser ~~operated in the TEM_{00} mode~~, we are suspending highly absorbing spherical carbon particles. This seems to be in total disagreement with our understanding of the radiometric force on a spherical particle, since for a Gaussian laser intensity profile the particle

Contd

should be pushed out of the beam. To the best of our knowledge this is the first report of an absorbing particle being stably trapped in a beam of light for which external conditions have not been tailored to counteract the preferred direction of migration.

In this communication we present the experimental observations and point out the physical mechanism that perhaps explains the phenomenon. Some of the possible implications of these results are then discussed with regard to providing a means for testing the electromagnetic diffraction theory of optical systems and to possible consequences of using laser beams for a variety of applications.

II. EXPERIMENTAL DESCRIPTION AND OBSERVATIONS

A schematic of the apparatus is shown in Fig. 1. It consists of an evacuable glass cell with removable CaF_2 windows at the bottom and the top. All experiments were performed with the cell at atmospheric pressure except for pressure dependence tests noted in the text. Another CaF_2 window allows viewing into the cell at a 45 deg angle. A continuous wave (cw) Nd:YAG laser, $\lambda = 1.06$ μm, operated in the TEM_{00} mode with linear polarization is directed into the cell from the bottom. The laser beam is expanded to a 5 mm diameter and focussed inside the cell with a 50 mm focal length CaF_2 lens. A 40 power magnification telemicroscope in conjunction with an IR viewer, which produces a visible image that is displayed on a video screen, is used for observing the particles. Some of the figures shown below are photographs of the video display. Aerosols are introduced into the beam by depositing a few on the inside of the top window and then tapping the window to release them. An electron microscope photograph of the spherical carbon particles used is shown in Fig. 2; the radii of these particles range from 0.75 to 4.0 μm.

Figure 3 is a photograph of a spherical carbon particle stably levitated using a laser beam with a photon flux at the focal plane of $\sim 10^3$ W/cm^2. The particle is trapped very near the focal plane. Our experience with single, electrostatically levitated carbon particles shows that spherical particles are a steady source of scattered radiation. Nonspherical particles, on the other hand, if illuminated with a laser are observed to twinkle. Monitoring the levitated particles in this experiment with both IR and visible radiation confirmed that the stably trapped particles are spherical and that no clumping together of particles is taking place.

Particulates have been suspended with laser beam intensities ranging from $\sim 10^2$ to 10^5 W/cm^2; their localization in the beam from particle to particle remains nearly constant, with the largest variation being ~ 0.5 mm. After a particle is trapped, varying the laser power from one extreme to the other causes it to move up or down by a few tenths of a millimeter. Also, the increase in intensity results in a more stably trapped particle; i.e., at the

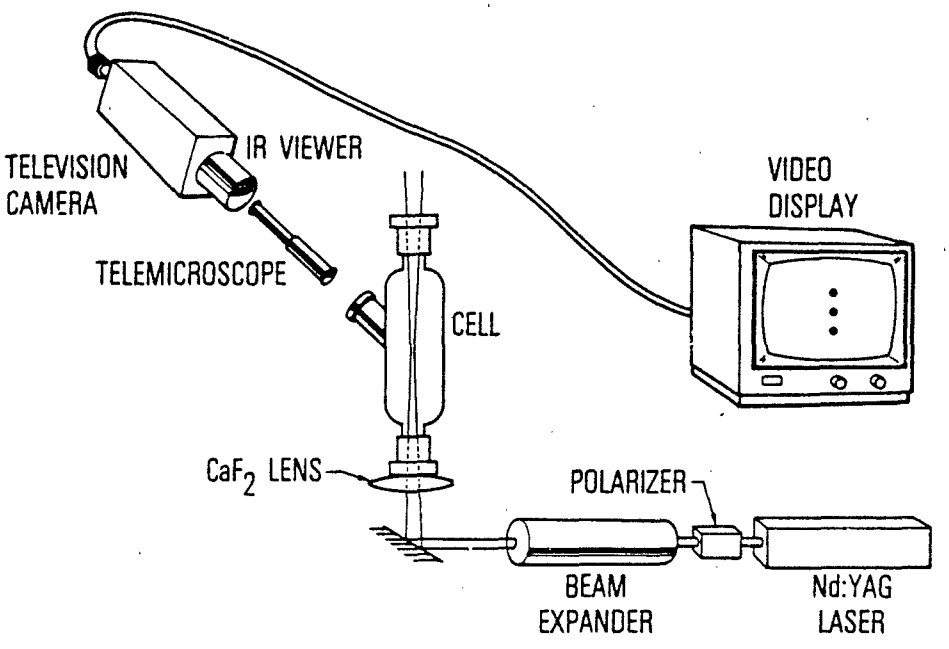

Fig. 1. Diagram of experimental apparatus used to trap and observe absorbing carbon microspheres.

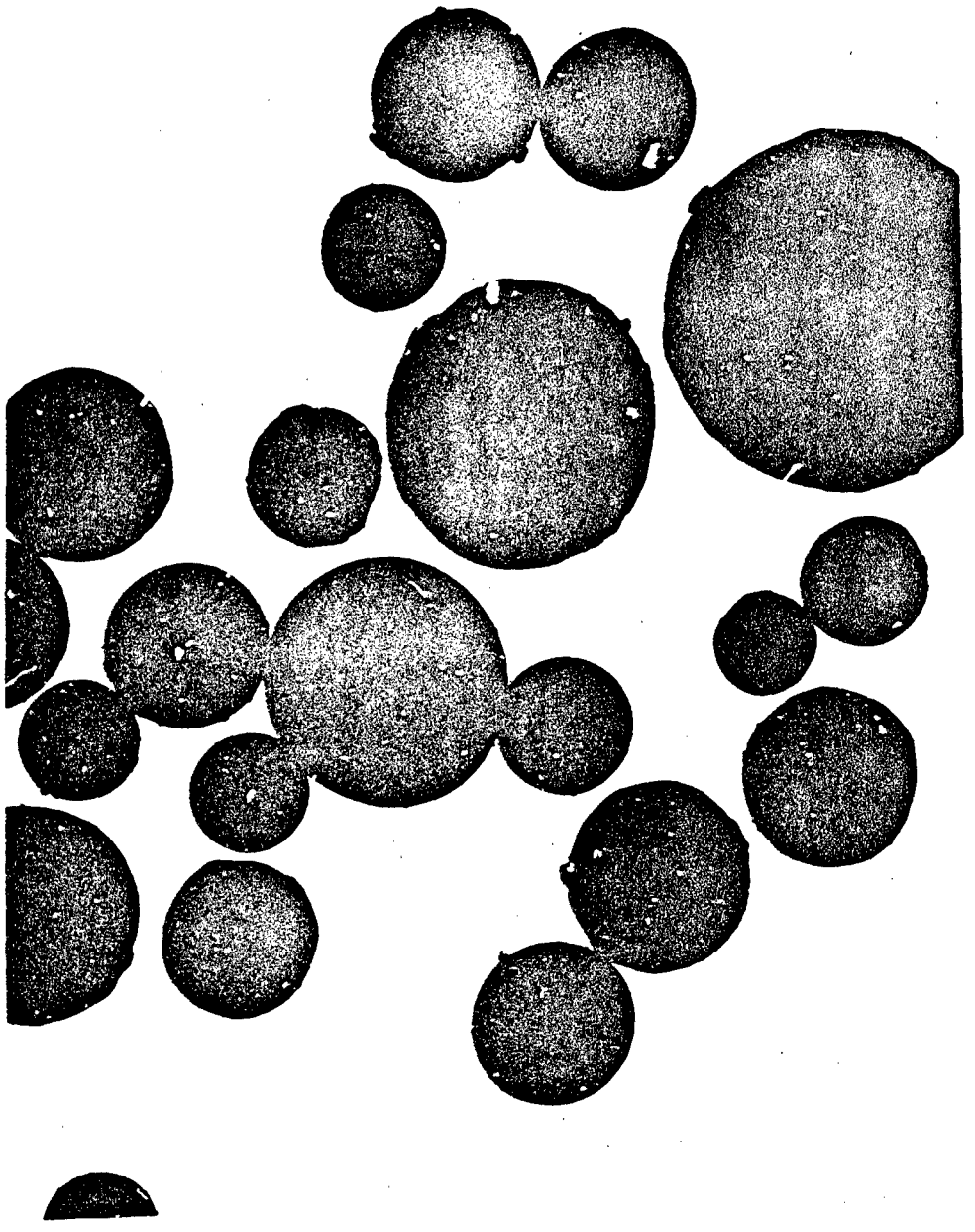

Fig. 2. Electron microscope photograph of spherical carbon particles used in the experiment. The radii range from 0.75 to 4.0 μm.

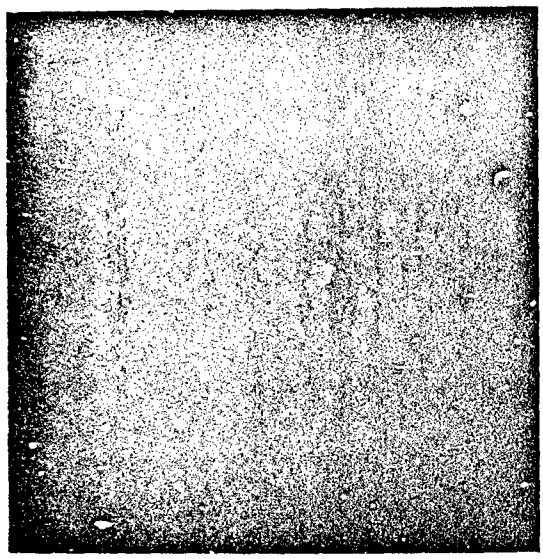

Fig. 3. A single carbon particle trapped near the focal plane.

lower power the particle exhibits jitter with amplitude a fraction of its size in all directions, but as the intensity is increased the jitter decreases.

If numerous particles are sprayed into the cell we observe some of the complex migrations mentioned above. In addition, a number of particles remain trapped above and below the focal plane; however, we have observed a pattern in the way they become suspended. The trapping of particles above the focal plane markedly increases when a particle is caught near the focal plane. Figure 4 shows two suspended particles; the distance between them is ~ 0.5 mm. Six levitated carbon aerosol particles are shown in Fig. 5. Using an auxiliary hand-held IR viewer, we have observed that there are actually many more trapped along the beam not seen in this figure because of the limited area viewed with the telemicroscope.

The experiment has been repeated with the laser directed down into the cell from the top and sideways by rotating the apparatus so that the optical axis is parallel to the table. These different experimental configurations produced the same results: stable suspension of carbon aerosol particles. It seems, therefore, that gravity and convection are not necessary influences for the levitation of particles. The mechanism is entirely particle, laser beam and surrounding-gas molecule dependent.

We have also performed the experiment using Al_2O_3 micron-sized spherical particles. Under the exact conditions as were used for the highly absorbing carbon particles, the weakly absorbing alumina particles were not trapped.

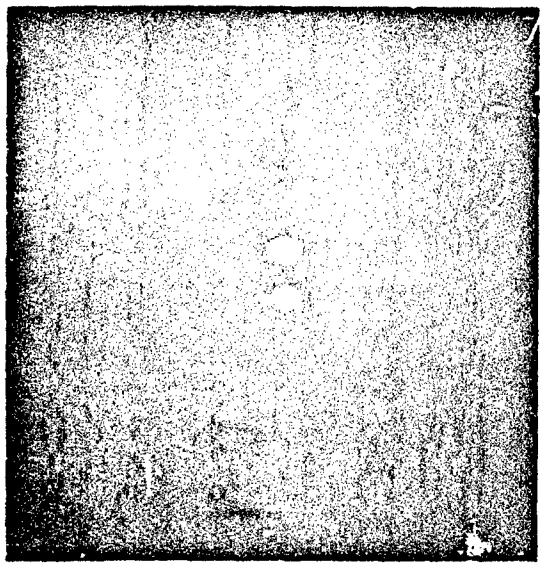

Fig. 4. Two carbon particles trapped near the focal plane. The separation between particles is ~ 0.5 mm.

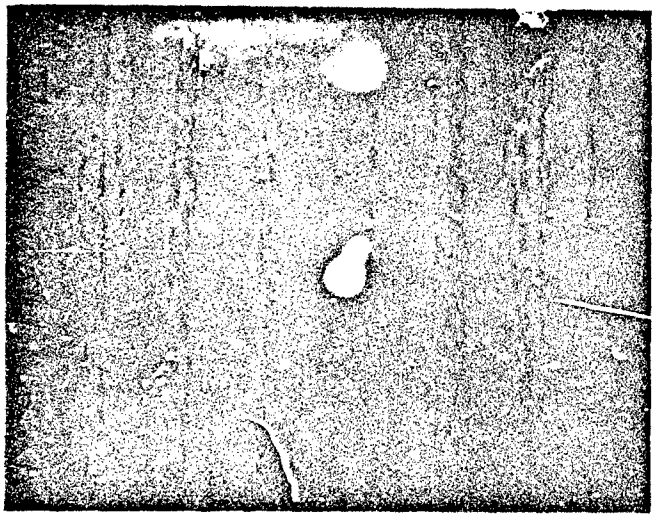

Fig. 5. Six carbon particles trapped above the focal plane.

III. THEORY AND CALCULATIONS

For low Knudsen number, i.e., particle sizes much larger than the mean free path of ambient gas molecules, we have recently shown[6] that the theory of Yalamov et al.[7] is valid for calculating the photophoretic force on a micron-sized particle. The expression for the force is

$$\vec{F} = \frac{-4\pi R \eta^2 K \vec{I} J}{\rho T \chi} \qquad (1)$$

where η, ρ, and T are, respectively, the viscosity, density, and temperature of the gas, and K is the thermal slip factor of the gas as it slides over the particle surface. The particle's radius and thermal conductivity are denoted by R and χ, and I is the irradiating intensity. The anisotropy factor J is a measure of the magnitude of the force and determines its direction; a negative J results in a force that pushes the particle away from the light source along the axis of propagation.

For gas viscosity $\eta = 2.95 \times 10^{-4}$ g/sec cm, particle thermal conductivity $\chi = 0.28$W/cm K, using standard temperature and pressure, and taking the thermal slip factor[8] to be K = 1.27, we calculate the force on a carbon particle irradiated with $I = 1 \times 10^3$ W/cm^2 plane wave. The resulting force is presented in Fig. 6 as a function of particle radius. For a 1 μm particle this force is ~ 2 orders of magnitude higher than that due to gravitation and radiation pressure. We see that the highly absorbing carbon particles are pushed away from the light source. The radiation-particle-interaction picture that emerges for carbon is that the spherical particle moves in a direction which is opposite to the surface that is irradiated; therefore, for a Gaussian intensity distribution we would expect the particle to move along the optical axis and to have a finite force component normal to the beam pushing it out of the laser. This physical picture is corraborated by the levitation of a dye-impregnated glycerol particle mentioned above where the absorbing particle is pushed towards the intensity minimum. What we observe in our experiment is in apparent contrast with this mechanism. However, a closer inspection of the

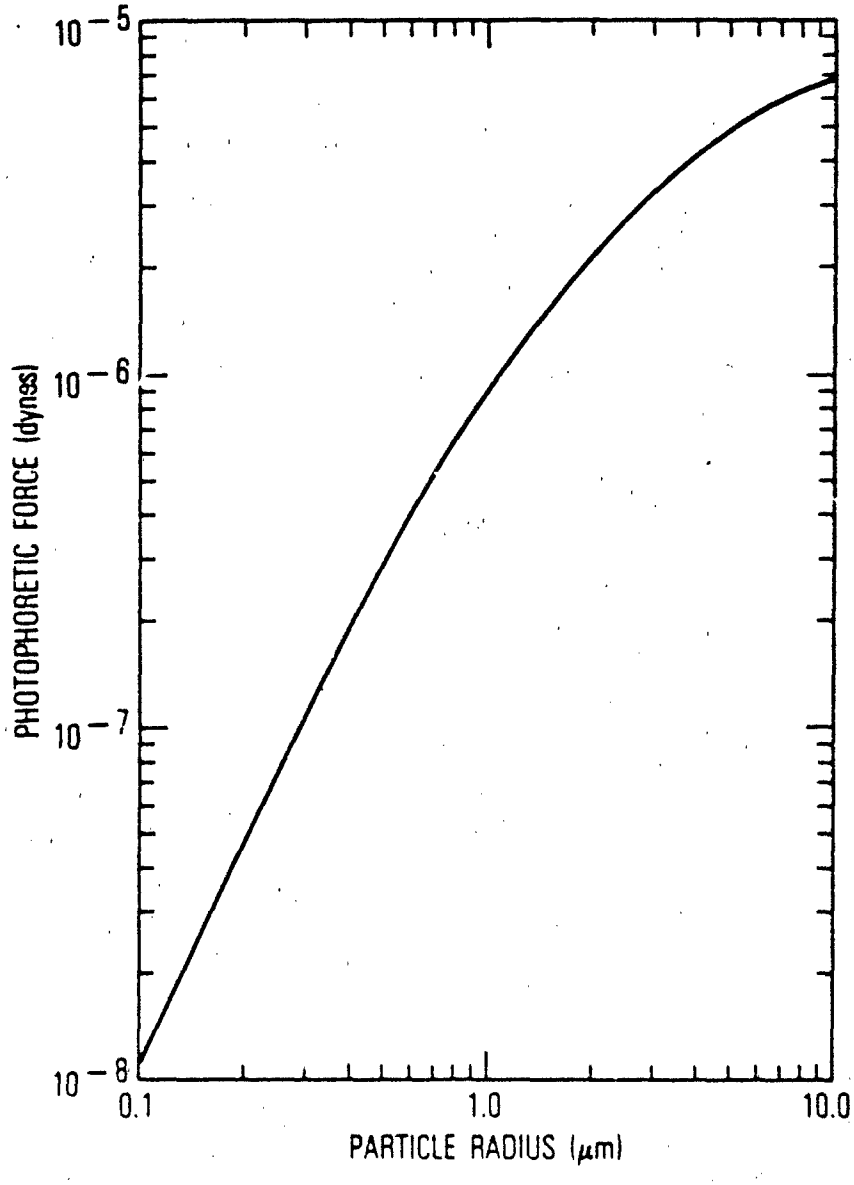

Fig. 6. Calculated photophoretic force for a spherical carbon particle.

laser intensity profile near the focus and, more important, of the direction of energy flow reveals that no contradiction exists.

After more than 60 years of experimental observations we can, finally, not only quantitatively predict the motion of a photophoresis driven spherical particle, but can use this force to optically characterize the particulate.[6] If we can use this understanding to learn about the particle, then the next step is a usage that reveals properties of the irradiating beam not easily observed on a microscopic scale by other means. Specifically, we are referring to microscopic spatial structures and localized vectorial features of focussed laser beams.

We use the theory developed by Wolf et al.[9-12] for calculating the electromagnetic diffraction of an optical system, modified to treat a Gaussian intensity distribution, to calculate the structure of the electromagnetic field near the focal region. The calculations are performed for the experimental conditions presented above, namely, a laser beam, $\lambda = 1.06$ μm, passing through a 5 mm aplanatic aperture, with a 100 mm radius of curvature. A three dimensional representation of the time-averaged energy density distribution near the focal plane, showing a slice through the center of the beam, is presented in Fig. 7. The electric field is parallel to the plane shown. We see that the energy density is highly structured and exhibits maxima and minima on both sides of the focal plane. For the relatively small aperture in the experiment, which corresponds to a half angle aperture of 2.86 deg, calculation of the time-averaged electric energy density performed with the electric field parallel, perpendicular and at 45 deg, resulted in the same distribution as is presented in Fig. 7 with the magnitude cut in half. Consequently, for our experimental configuration, the electric energy density is independent of the azimuthal angle, and the contours of constant energy density are rings around the optical axis. Furthermore, at the focal plane the positions of the bright and dark rings closely correspond to the Airy diffraction pattern. If we imagine rotating Fig. 7 about the optical axis, we see that there are small volumes near the focal plane that are at lower energy levels. These low energy density volumes of themselves cannot account for the trapping of particles. We have established that a photophoresis-driven spherical carbon

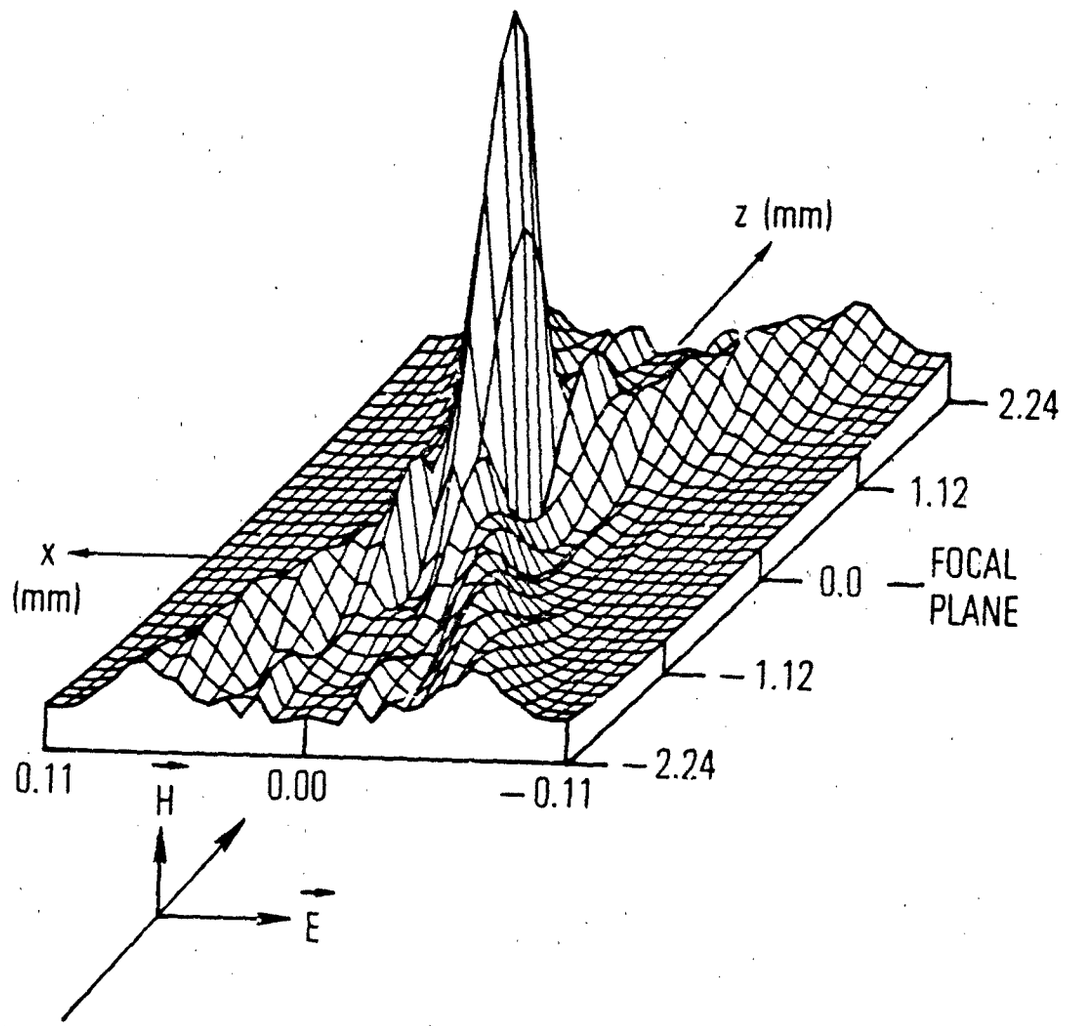

Fig. 7. Three dimensional plot of time-averaged electromagnetic energy density near the focal plane for a slice through the center of the laser beam.

particle moves in a direction which is opposite to the surface that absorbs the light. Therefore, if the energy flow is simply diverging for positive z-coordinate values the particle should continue to move along these lines of flow even if it goes through a region of lower energy density. At this point it could be argued that the particle is caught inside an energy density well; this, of course, is a possibility for the laser pointed up experiment. However, we have shown that gravity is not necessary for trapping particles; the responsible mechanism must provide a stabilizing force in all directions that keeps the particle trapped in a small volume of space.

The formalism developed in Refs. 9-12 goes beyond the usual scalar diffraction theories and presents a method for calculating the vectorial features of the field near the focus. We use this representation to calculate the Poynting vector for the same geometry and coordinates used above. Figure 8 presents the tangents to the energy flow lines passing through each point. For the most part the beam converges to the focal plane and then diverges; however, there are regions where the energy flow is sharply directed away from this general trend. A blow-up of the x = 8.45 to 11.15 μm, z = 1080 to 1140 μm region by a factor of 30 reveals some of the complexities in the flow. The arrows in Fig. 9 are the calculated directions of the Poynting vector at the particular coordinates; to help visualize the energy flow, the dotted lines were drawn in. For an aplanatic system, this flow is quite involved. Contrary to our usual notions, Ignatowsky, in 1919, deduced that there are regions where the flow is directed back toward the object.[10] The more recent detailed calculations of Ref. 12 show the flow of energy actually whirling around at the focal plane. Our calculations, as can be seen in Figs. 8 and 9, reveal a swirling motion for $z > 0$. In addition, these results indicate that local maxima in the intensity are accompanied by converging energy flow toward that point. Contours of constant energy density are represented by the solid lines in Fig. 9a and the three dimensional representation of this same region is shown below in Fig. 9b. For a carbon particle located at x = 9.125 μm and z = 1120 μm any motion toward the forward direction is halted by the higher flux of photons intercepted by the rear half of the particle. The photons do not have to be directed back toward the source; it

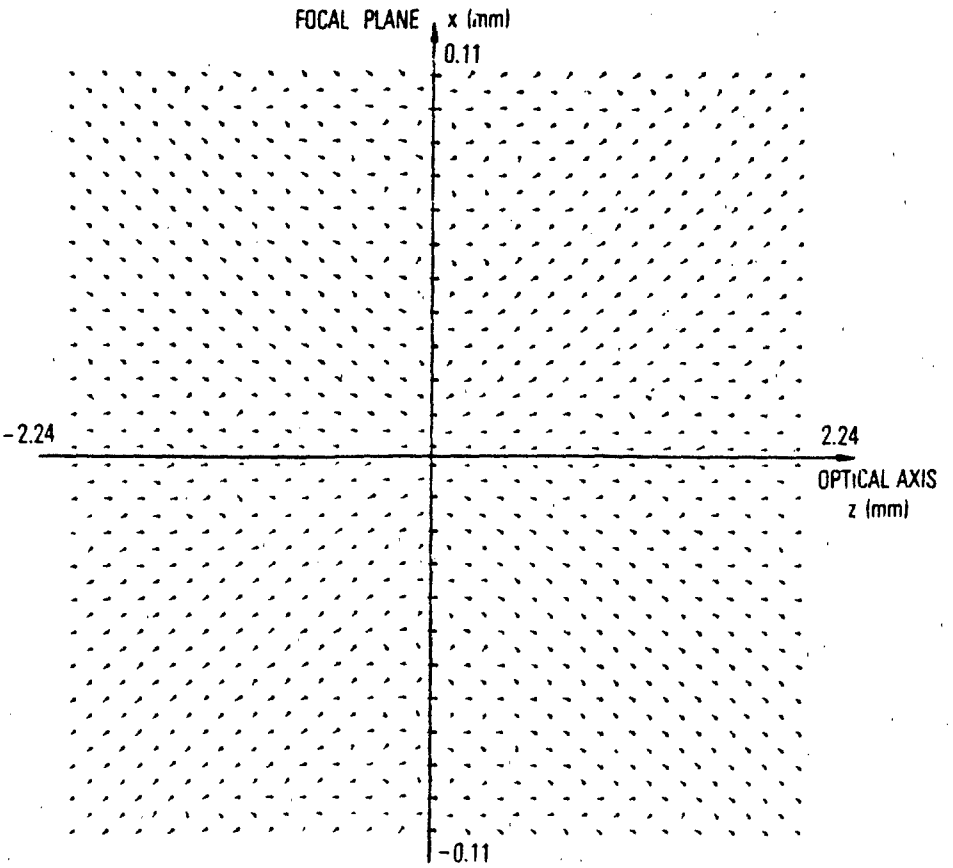

Fig. 8. Direction of Poynting vector near the focus. Arrows represent tangent to energy flow line passing through each point.

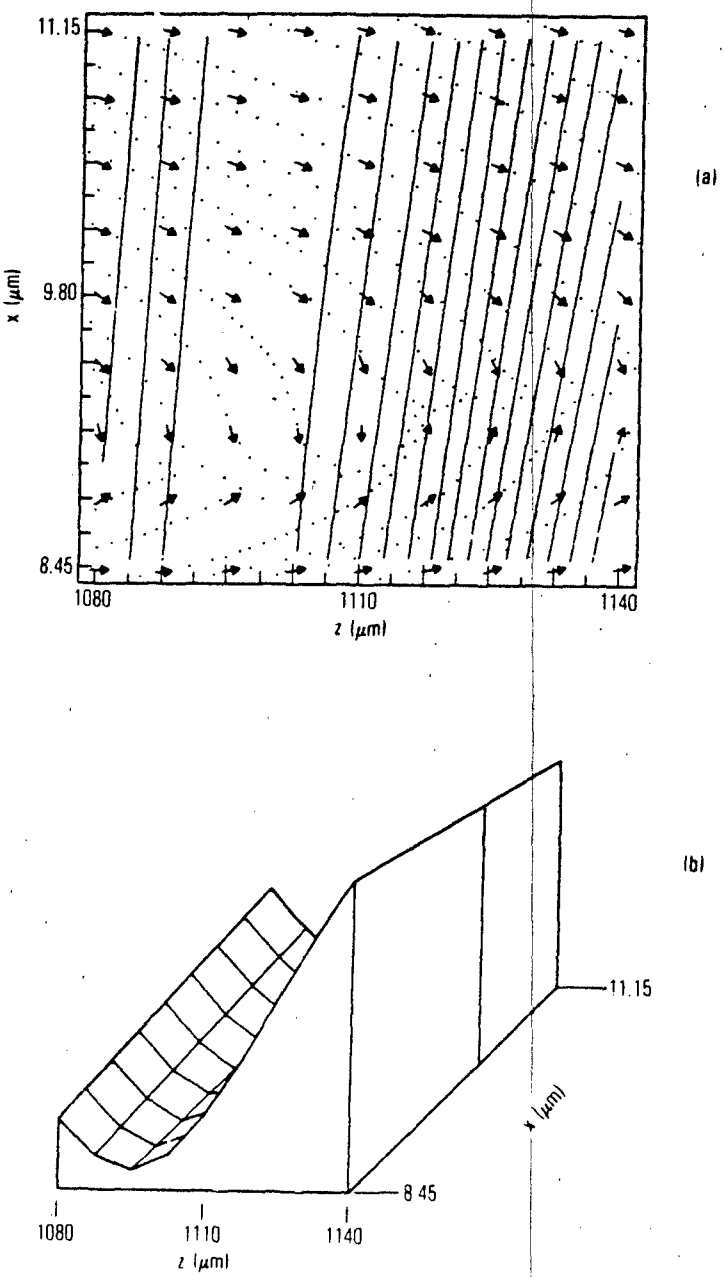

Fig. 9. Blow-up of x = 8.45 to 11.15 μm; z = 1080 to 1140 μm region: (a) direction of Poynting vector and contours (solid lines) of constant electric energy density; (b) three dimensional plot of electric energy density.

is only important that the rear half absorb more energy. The removal of this energy by the surrounding gas molecules imparts a force on the particle considerably greater than that due to photon momentum and is directed normal to the surface. The mechanism is schematically summarized in Fig. 10. With this pictorial insight it is easy to visualize a carbon particle "falling" into one of these energy density "holes" and becoming trapped. The observation that the number of particles trapped increases after one is suspended suggests that the electromagnetic field is further disturbed by the particle to form more intensity minima and swirling in the energy flow, which, in turn, cause more particles to be suspended and so on.

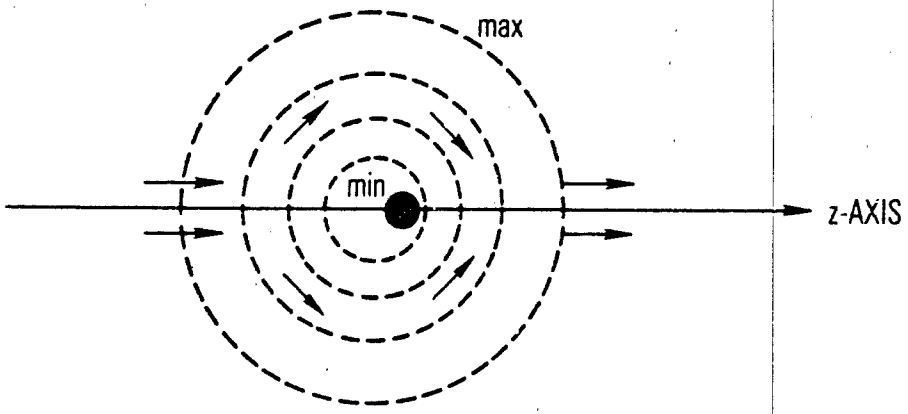

Fig. 10. Schematic representation of mechanism responsible for trapping a particle.

IV. DISCUSSION AND CONCLUSION

We have shown that absorbing spherical carbon aerosol can remain suspended in the volume swept by a focussed CW Nd:YAG laser. Convection, resulting from the heating of any part of the cell, as a possible levitating mechanism was eliminated by reproducing the same results with the beam entering the cell from the top and sideways. The two remaining known possible forces are radiation pressure and photophoresis. Since for an absorbing particulate the force due to the photon momentum is negligible compared to the radiometric force, photophoresis emerges as the only possible candidate. From Eq. (1) we see that the photophoretic force can be investigated by lowering the pressure inside the cell, or by increasing the photon flux. In both cases the particles should be displaced accordingly. Our experiments did not show a proportional displacement. We have argued that this behavior is due to the particle being surrounded by regions of higher energy density and swirling energy flow; a move towards a more intense part of the beam causes the rear part of the particle to absorb more energy, resulting in an anisotropic gas reaction that pushes the particle back. This is totally in accord with the experimental observations that particles can be trapped with the laser beam pointed in any direction and that the jitter decreases when the power is increased. The jitter decreases because the increasing intensity shrinks the volume that can be occupied by the particle and constrains movement.

The spatial variations of the electromagnetic field near the focus have been measured for a microwave beam by Carswell.[13] Our experiment is, we believe, the first to probe the microscopic spatial structure of the field that seems, if our conjecture is borne out, to furnish experimental proof of the complex vectorial features of the energy flow due to diffraction effects. For applications of practical interest most electromagnetic diffraction theories are approximate representations of the physical interaction. Our observations seem to indicate that an absorbing micron-sized particle, perhaps electrostatically suspended as in Ref. 5, could be used to investigate the complex structure of a diffracted laser beam by directly prob-

ing the spatial variations in the near, because of the relatively low power required, as well as the far field. These types of studies could have some bearing in the development and testing of new, rigorous diffraction theories and in applications where the focusing of laser beams to small spot sizes are important, e.g., laser fusion, multiphoton absorption, and nonlinear optics.

Regardless of the mechanism responsible, these results point out that relatively low power lasers used in an aerosol environment can trap absorbing particles. Therefore, applications such as laser communication, among others, cannot assume that the distribution and motion of aerosol in the volume swept by the laser is independent of the laser itself. Calculations assuming aerosol distribution independent of laser-particle interaction might be overestimating the transmission.

REFERENCES

1. A. Ashkin, Phys. Rev. Lett. 24, 156 (1970).

2. A. Ashkin and J. M. Dziedzic, Appl. Opt. 19, 660 (1980).

3. O. Preining, in Aerosol Science, C. W. Davies, ed. (Academic, New York, 1966).

4. N. A. Fuchs, The Mechanics of Aerosols (Pergamon, New York, 1964).

5. M. Lewitts, S. Arnold and G. Oster, Appl. Phys. Lett. 40, 455 (1982).

6. A. B. Pluchino, Appl. Opt. 22, 103 (1983).

7. Yu. I. Yalamov, V. B. Kutukov and E. R. Shchukin, J. Colloid Interface Sci. 57, 564 (1976).

8. V. B. Derjaguin and Yu. I. Yalamov, in International Reviews in Aerosol Physics and Chemistry, V3, G. M. Hidy and J. R. Brock, eds. (Pergamon, New York, 1972).

9. E. Wolf, Proc. Roy. Soc. A253, 349 (1959).

10. B. Richards and E. Wolf, Proc. Roy. Soc. A253, 358 (1959).

11. A. Boivin and E. Wolf, Phys. Rev. 138, B1561 (1965).

12. A. Boivin, J. Dow and E. Wolf, J. Opt. Soc. Am. 57, 1171 (1967).

13. A. I. Carswell, Phys. Rev. Lett. 15, 647 (1965).

☆U.S. GOVERNMENT PRINTING OFFICE: 1986—678—004/30423

LABORATORY OPERATIONS

The Aerospace Corporation functions as an "architect-engineer" for national security projects, specializing in advanced military space systems. Providing research support, the corporation's Laboratory Operations conducts experimental and theoretical investigations that focus on the application of scientific and technical advances to such systems. Vital to the success of these investigations is the technical staff's wide-ranging expertise and its ability to stay current with new developments. This expertise is enhanced by a research program aimed at dealing with the many problems associated with rapidly evolving space systems. Contributing their capabilities to the research effort are these individual laboratories:

Aerophysics Laboratory: Launch vehicle and reentry fluid mechanics, heat transfer and flight dynamics; chemical and electric propulsion, propellant chemistry, chemical dynamics, environmental chemistry, trace detection; spacecraft structural mechanics, contamination, thermal and structural control; high temperature thermomechanics, gas kinetics and radiation; cw and pulsed chemical and excimer laser development including chemical kinetics, spectroscopy, optical resonators, beam control, atmospheric propagation, laser effects and countermeasures.

Chemistry and Physics Laboratory: Atmospheric chemical reactions, atmospheric optics, light scattering, state-specific chemical reactions and radiative signatures of missile plumes, sensor out-of-field-of-view rejection, applied laser spectroscopy, laser chemistry, laser optoelectronics, solar cell physics, battery electrochemistry, space vacuum and radiation effects on materials, lubrication and surface phenomena, thermionic emission, photosensitive materials and detectors, atomic frequency standards, and environmental chemistry.

Computer Science Laboratory: Program verification, program translation, performance-sensitive system design, distributed architectures for spaceborne computers, fault-tolerant computer systems, artificial intelligence, microelectronics applications, communication protocols, and computer security.

Electronics Research Laboratory: Microelectronics, solid-state device physics, compound semiconductors, radiation hardening; electro-optics, quantum electronics, solid-state lasers, optical propagation and communications; microwave semiconductor devices, microwave/millimeter wave measurements, diagnostics and radiometry, microwave/millimeter wave thermionic devices; atomic time and frequency standards; antennas, rf systems, electromagnetic propagation phenomena, space communication systems.

Materials Sciences Laboratory: Development of new materials: metals, alloys, ceramics, polymers and their composites, and new forms of carbon; nondestructive evaluation, component failure analysis and reliability; fracture mechanics and stress corrosion; analysis and evaluation of materials at cryogenic and elevated temperatures as well as in space and enemy-induced environments.

Space Sciences Laboratory: Magnetospheric, auroral and cosmic ray physics, wave-particle interactions, magnetospheric plasma waves; atmospheric and ionospheric physics, density and composition of the upper atmosphere, remote sensing using atmospheric radiation; solar physics, infrared astronomy, infrared signature analysis; effects of solar activity, magnetic storms and nuclear explosions on the earth's atmosphere, ionosphere and magnetosphere; effects of electromagnetic and particulate radiations on space systems; space instrumentation.